HIGH FREQUENCY CURRENT DISTRIBUTION IN A STRUCTURE WITH APPLICATION TO LIGHTNING PROTECTION SYSTEMS

Andrew Graham Swanson

A research report submitted to the faculty of Engineering and the Built Environment, University of the Witwatersrand, in fulfilment of the requirements for the degree of Master of Science of Engineering

Johannesburg, August 2, 2006

Abstract

In concrete reinforced buildings, the steel framework is required to be bonded and is often used as a cost effective method of lightning protection. In defining lightning protection zones, it is essential to understand where the lightning current due to a direct strike will flow. A number of models exist to evaluate the current distribution, but are often applied to relatively simple structures.

Using Maxwell's equations, an approximate skin effect model is proposed and used to evaluate the lightning current distribution in a complex structure. A reduced scale model of a structure, consisting of conductors arranged in rings, is developed to verify the model. Particular attention is given to the return path of the current, ensuring an even distribution of the current in the structure.

The equivalent circuit showed an even distribution of current across each conductor at dc and low frequencies and a distribution that concentrated in the outer conductors for higher frequencies. The measurements from the structure confirmed that the current concentrates in the outer conductors at high frequencies. Applying a reduced scale lightning impulse, it is shown that the majority of the current flows on the outermost conductors. Any current on the inner conductors is not only greatly decreased in magnitude, but significantly slower in time than the applied impulse.

Declaration

I declare that this dissertation is my own, unaided work. It is being submitted for the Degree of Master of Science in the University of the Witwatersrand, Johannesburg. It has not been submitted before for any degree or examination in any other University.

Signed on August 2, 2006

Andrew Graham Swanson

Acknowledgements

Contents

List of Figures

List of Tables

List of Symbols

δ	Skin depth [m], *Equation (1), pg 1.*
f	Frequency [Hz], *Equation (1), pg 1.*
μ_0	Permeability of free space [$4\pi \times 10^{-7}$ H.m^{-1}], *Equation (1), pg 1.*
μ_r	Relative permeability, *Equation (1), pg 1.*
σ	Conductivity [S.m^{-1}], *Equation (1), pg 1.*
$\mathbf{E}$	Electric field [V.m^{-1}], *Equation (2), pg 2.*
$\mathbf{H}$	Magnetic field [A.m^{-1}], *Equation (2), pg 2.*
I	Enclosed current [A], *Equation (3), pg 2.*
r	Radius from the centre of the conductor [m], *Equation (3), pg 2.*
r_i	Radius of ring i [m], *Equation (5), pg 2.*
E_i	Electric field at ring i [V.m^{-1}], *Equation (5), pg 2.*
I_i	Enclosed current at ring i [A], *Equation (5), pg 2.*
J_i	Current density between rings i and $i+1$ [A.m^{-2}], *Equation (6), pg 2.*
ω	Angular frequency [rad.s^{-1}], *Equation (7), pg 2.*
ϵ_0	Permittivity of free space [8.85×10^{-12} F.m^{-1}], *Equation (7), pg 2.*
A_i	Area between rings i and $i+1$ [m^2], *Equation (8), pg 2.*
R_i	Partial resistance [Ω.m^{-1}], *Equation (9), pg 2.*
L_i	Partial inductance [H.m^{-1}], *Equation (10), pg 2.*
C_i	Partial capacitance [F.m^{-1}], *Equation (11), pg 2.*
Δr	Difference between rings ($r_i - r_{i+1}$) [m], *pg 2.*
k_c	Current partioning coefficient, *Equation (B.1), pg 12.*
I_k	Partition of current [A], *Equation (B.1), pg 12.*
I_t	Input current [A], *Equation (B.1), pg 12.*
k_1	Emperical current partioning coefficient, *Equation (B.2), pg 12.*

n	Number of down conductors, *Equation (B.2), pg 12.*
c	Distance to closest down conductor [m], *Equation (B.2), pg 12.*
h	Height of down conductor [m], *Equation (B.2), pg 12.*
q	Scale factor, *Equation (C.1), pg 14.*
l	Length of the scaled model [m], *Equation (C.1), pg 14.*
l'	Length of the full scale model [m], *Equation (C.1), pg 14.*
$\mathbf{J}$	Current density [A.m^{-2}], *Equation (D.1), pg 17.*
J_0	Current density at the surface [A.m^{-2}], *Equation (D.1), pg 17.*
x	Distance from the conductor surface [m], *Equation (D.1), pg 17.*
$\mathbf{A}$	Magnetic vector potential [Wb.m^{-1}], *Equation (D.3), pg 18.*
$\mathbf{\Phi}$	Electric scalar potential [J.C^{-1}], *Equation (D.3), pg 18.*
$V_j - V_k$	Voltage across branch [V], *Equation (D.7), pg 19.*
R_n	Resistance [Ω], *Equation (D.7), pg 19.*
L_{pnn}	Self inductance of branch n [H], *Equation (D.7), pg 19.*
I_{Ln}	Current in branch n [A], *Equation (D.7), pg 19.*
L_{pn}	Mutual inductance of branch m [H], *Equation (D.7), pg 19.*
I_{Lm}	Current in branch m [A], *Equation (D.7), pg 19.*
L_{pmk}	Partial inductance [H], *Equation (D.8), pg 19.*
L_{pskk}	Partial self inductance [H], *Equation (D.8), pg 19.*
β	Propagation constant, *Equation (D.8), pg 19.*
l_k	Length of the conductor [m], *Equation (D.8), pg 19.*
L_{psmk}	Partial mutual inductance [H], *Equation (D.8), pg 19.*
$\lvert r_k - r_m \rvert$	Distance between segments [m], *Equation (D.8), pg 19.*
λ	Magnetic flux linkage [Wb.m^{-1}], *Equation (F.2), pg 28.*
n	Number of turns per metre, *Equation (F.2), pg 28.*

A	Area of coil [m^2], *Equation (F.2), pg 28.*
i	Conductor current [A], *Equation (F.2), pg 28.*
v	Voltage of coil [V], *Equation (F.3), pg 28.*
N	Number of turns, *Equation (F.3), pg 28.*
l	Length of the coil [m], *Equation (F.3), pg 28.*
I_{in}	Input/reference current [A], *Equation (G.1), pg 31.*
f_0	Frequency of waveform [Hz], *Equation (G.1), pg 31.*
t	Time [s], *Equation (G.1), pg 31.*
I	Lightning impulse current [A], *Equation (G.2), pg 33.*
I_{peak}	Peak current [A], *Equation (G.2), pg 33.*
t	Time [μs], *Equation (G.2), pg 33.*
τ_f	Front time [μs], *Equation (G.2), pg 33.*
τ_t	Tail time [μs], *Equation (G.2), pg 33.*
n	Exponential factor, *Equation (G.2), pg 33.*

Preface

This research report presents the work in the form of a short paper, followed by a number of appendices. The paper proposes the current distribution model and presents a discussion on the results obtained. The appendices provide a more in depth explanation of the work covered, where each appendix is referenced seperately. A short description of the appendices follows.

Appendix A - Lightning Stroke Parameters - defines the lightning short stroke parameters as given in the IEC Standard 62305-1.

Appendix B - Lightning Protection - presents an overview of lightning protection, with emphasis on internal lightning protection and the definition of lightning protection zones. The empirical current distribution and its limitations are also presented.

Appendix C - Geometric Modelling - presents a review of studies on the reduced scale modelling of structures and reviews the use of scale factors in reduced scale laboratory experiments.

Appendix D - Modelling - provides an overview of proposed models to simulate the response of structures to a direct lightning strike. The partial element equivalent (PEEC) model and the skin effect model for a circular conductor. The latter is extended to include non-conductive layers.

Appendix E - Experimental Setup - presents the reduced scale model of a structure used to verify the results from the skin effect equivalent circuit.

Appendix F - Measurement System - presents the measurement system with emphasis on Rogowski coils and their use for measurement of time-varying currents.

Appendix G - Results - presents the equivalent circuit of the proposed model and the results of the simulation, including the magnitude response and phase angle of each conductor ring. A lightning impulse is applied to the circuit and the results are presented. The response of each conductor ring of the physical structure is measured and the results presented.

HIGH FREQUENCY CURRENT DISTRIBUTION IN A STRUCTURE WITH APPLICATION TO LIGHTNING PROTECTION SYSTEMS

Andrew Graham Swanson

School of Electrical and Information Engineering, University of the Witwatersrand, Johannesburg, South Africa.

Abstract: A number of models to evaluate the current distribution in a structure exist. Based on the fact that these models are not used on complex structures such as reinforced concrete structures, an equivalent circuit, based on Maxwell's equations, is proposed. A lightning impulse is applied to the circuit and it is shown that the majority of current flows in the outer conductor ring, due to the high frequency nature of lightning.

Keywords: Lightning protection, skin effect equivalent circuit, conductor rings, scale modelling

1 Introduction

The purpose of lightning protection is to prevent or reduce the risk of damage to equipment, loss of service or loss of life [1]. As part of effective and safe grounding, all metal objects are required to be bonded and electrically grounded [2]. In complex reinforced concrete structures, the steel re-bars provide additional down conductors [3].

Lightning protection zones are volumes of successively increasing protection against lightning electromagnetic waves and surges on incoming lines [1, 4]. In defining these zones the current distribution throughout the structure must be known.

A number of models are proposed to determine the distribution of current within the structure [5, 6, 7, 8]. These proposed models are, however, applied to simple systems without any justification into the exclusion of internal down conductors, as in the case of complex reinforced concrete structures.

A skin effect model for a coaxial line is extended to include non conducting layers and an equivalent circuit proposed. A structure to verify the model is constructed with particular attention given to the return path of the current, ensuring the even distribution of current within the conductor rings.

2 Skin Effect Model

The skin effect is the tendency for time varying currents to concentrate on the surface of the conductor. Skin depth is dependent on the frequency of the applied waveform and the electrical characteristics of the conductor [9]. Skin depth is given by [9]:

$$\delta = \frac{1}{\sqrt{2\pi f \mu_0 \mu_r \sigma}} \tag{1}$$

Where:
f = frequency [Hz]
μ_0 = permeability of free space [H.m^{-1}]
μ_r = relative permeability
σ = conductivity [S.m^{-1}]

Yen, Fazarinc and Wheeler propose an equivalent circuit to model the skin effect based on Maxwell's equations [10]. The model is developed for time domain analysis of transmission lines, which makes it suitable for lightning impulse analysis [10]. A conductor is divided into M concentric rings and a circuit model consisting of M partial resistors and $M-1$ partial inductors is developed [10]. The model is extended here to include non-conductive layers.

Faraday's law states that a changing magnetic field induces an electric field. In differential form, Faraday's law is given by [11]:

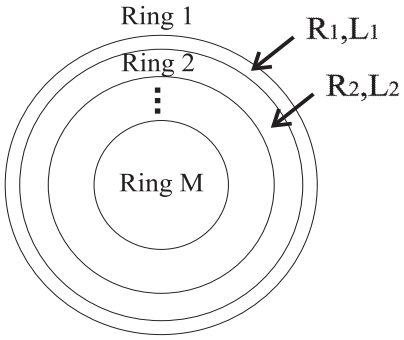

Figure 1: Concentric rings of a conductor

$$\nabla \times \mathbf{E} = -\mu \frac{\partial \mathbf{H}}{\partial t} \tag{2}$$

The line integral of the magnetic field is equal to the enclosed current [11]:

$$I(r,t) = 2\pi r H(r,t) \tag{3}$$

By substituting *Equation 3*, Faraday's law is rewritten:

$$\frac{\partial E(r,t)}{\partial r} = -\frac{\mu}{2\pi r}\frac{\partial I}{\partial t} \tag{4}$$

By dividing the conductor into M rings as shown in *Figure 1*, where $i = 1$ is the outermost ring and $i = M$ is the innermost ring, an approximate equation is given by:

$$E_{i-1} - E_i = \frac{\mu(r_{i-1} - r_i)}{2\pi r_i}\frac{dI_i}{dt} \tag{5}$$

The electric field at a point in a conductor is related to the current density by [11]:

$$E_i = \frac{J_i}{\sigma} \tag{6}$$

For a non conductive ring the displacement currents is related to the electric field by [11]:

$$E_i = \frac{J_i}{j\omega\epsilon} \tag{7}$$

Assuming the current density between rings is constant, the current density is equal to the difference between the enclosed currents divided by the area [10]:

$$J_i = \frac{I_i - I_{i+1}}{A_i} \tag{8}$$

The partial elements for the equivalent circuit shown in *Figure 2* are given by [10]:

$$R_i = \frac{1}{A_i\sigma} \tag{9}$$

$$L_i = \frac{\mu(r_{i-1} - r_i)}{2\pi r_i} \tag{10}$$

$$C_i = \frac{1}{\epsilon A_i} \tag{11}$$

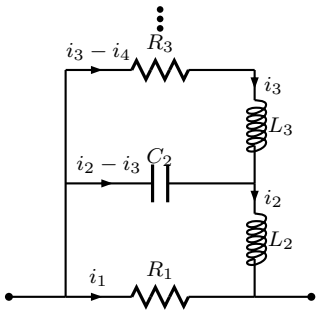

Figure 2: Skin effect equivalent circuit

These partial elements form parallel paths, approximating a solution for *Equation 4*. For direct current or low frequencies the current distribution is uniform, and the impedance reduces to the parallel combination of the resistors. At higher frequencies, the partial inductance causes the current to concentrate toward the outer rings. At very high frequencies, the current is limited to the resistance of the outermost ring, as there is no internal flux [10, 12].

For effective analysis over the full frequency domain the number of concentric rings must approach infinity, where Δr is smaller than the skin depth δ.

3 Experimental Setup

3.1 Test Structure

The test structure consists of a number of conductor rings arranged as shown in *Figure 3*. Copper plates provide equipotential platforms for the conductors at the top and on the base. The structure is constructed from non-ferrous materials to avoid the non linearities associated with the saturation and permeability of ferrous materials. The structure is intended as a 1:20 reduced scale model of a full scale structure.

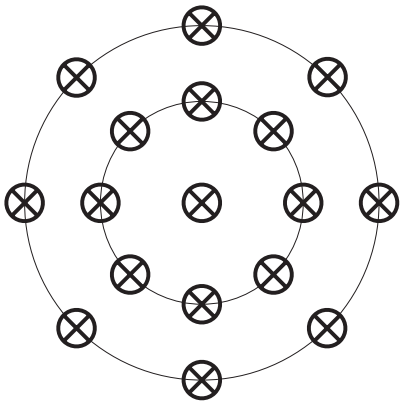

Figure 3: Down conductor ring arrangement

Table 1: Dimensions of the structure

Parameter	Value
Outer radius	14 cm
Inner radius	8.5 cm
Rod radius	3 mm

In high frequency applications, inductance is highly influential on the path of the current. For this reason aluminium mesh is used as the return path, as illustrated in *Figure 4*, as it provides an even distribution of current in the conductor rings [3, 13].

3.2 Measurement System

The measurement system consists of current probes in the form of Rogowski coils, which are connected to an oscilloscope by means of coaxial lines. All signal processing is done in MATLAB.

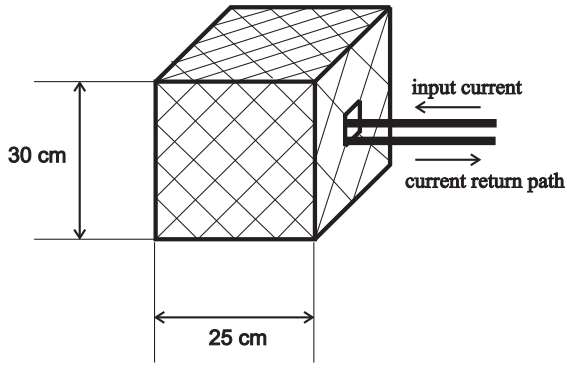

Figure 4: Aluminium mesh used as the return path for the current

The voltage output of a Rogowski coil is proportional to the rate of a change of current [14]:

$$v = -\frac{\mu_0 N A}{l}\frac{di}{dt} \tag{12}$$

The coils are sensitive to small currents, provided the frequency is sufficiently high. The coils and coaxial lines are not shielded and are subjected to electrostatic interference, because of the high $\frac{dV}{dt}$. Additional resonance is evident at 12.5 MHz.

4 Results

4.1 Measured results

Due to the even distribution of current within each conductor ring, a single conductor measurement from the outer and inner conductor rings represents $\frac{1}{8}$ of the total of each conductor ring current. Thus only four measurements are required the input current (I_{in}), the outer conductor current (I_1), the inner conductor current (I_2) and the centre conductor current (I_3).

The signals are filtered in MATLAB and are referenced to the input current such that:

$$I_{in} = sin(2\pi f_0 t) \tag{13}$$

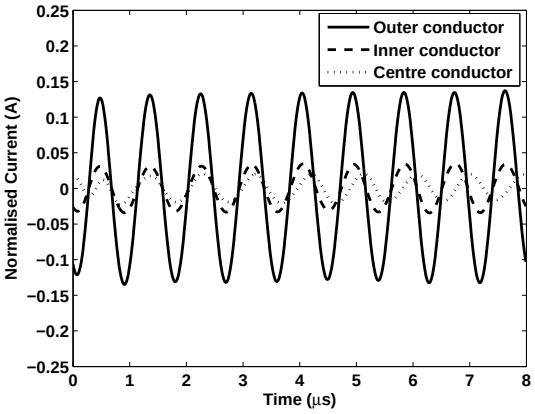

Figure 5: Current distribution in the time domain where $f_0 = 1.25$ MHz

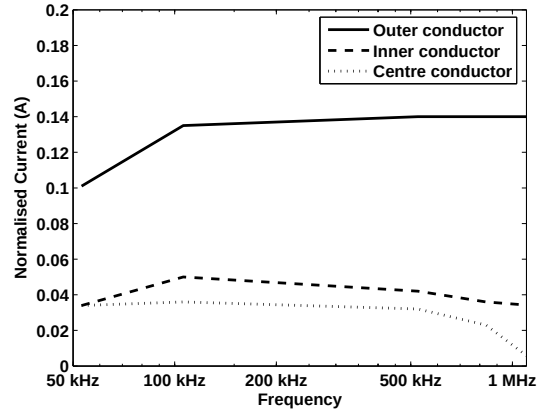

Figure 6: Magnitude response of the conductors in the frequency domain from $f_0 = 50$ kHz to $f_0 = 1.25$ MHz

4.2 Simulated results

A model consisting of 5 concentric rings is used to evaluate the current distribution in the structure. The equivalent circuit, shown in *Figure 7*, consists of:

- R_1, R_3 and R_5 representing the partial resistances of the conductor rings
- C_2 and C_4 representing the partial capacitances of the gaps between the conductor rings
- L_2 to L_4 representing the partial inductances of each ring.

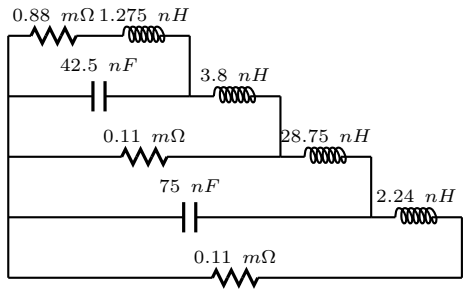

Figure 7: Approximate skin effect equivalent circuit

The magnitude response and phase angle of the 3 conductor rings are shown in *Figures* 8 and 9.

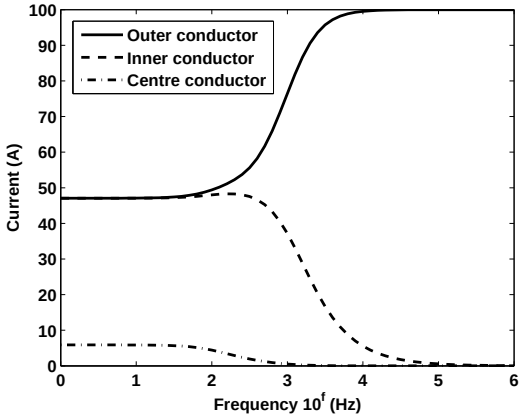

Figure 8: Magnitude response of the conductor rings

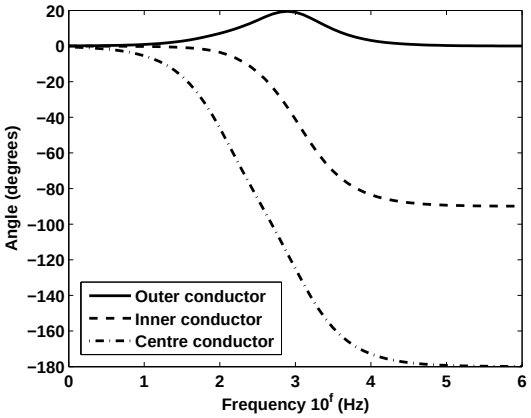

Figure 9: Phase angle of the conductor rings

The equivalent circuit model is a 1:20 reduced scale model of a structure; thus when applying a lightning current impulse, the impulse must be scaled accordingly [15]. The standard 5.5/75 μs lightning current impulse becomes a 0.3/3.75 μs impulse. A 100 A impulse is applied to the the circuit.

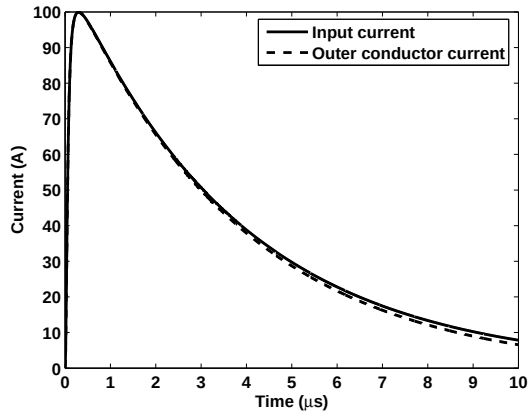

Figure 10: Impulse response of the outer conductor ring

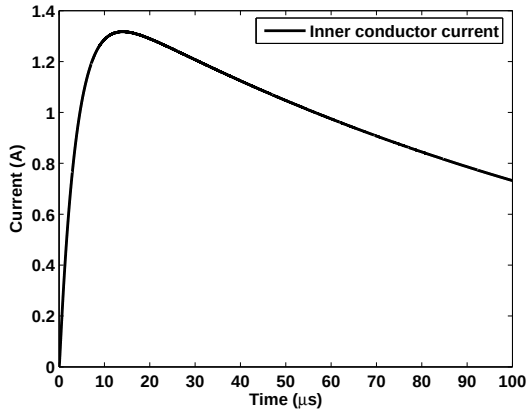

Figure 11: Impulse response of the inner conductor ring

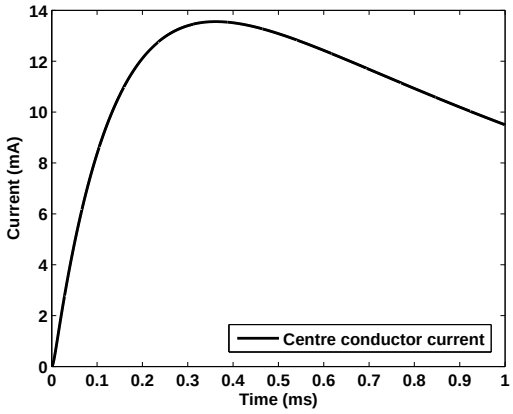

Figure 12: Impulse response of the centre conductor

5 Discussion

The measured results in *Figures* 5 and 6 confirm that the current concentrates on the outermost conductors and that the least current is found at the centre of the structure.

As discussed previously the outer and inner conductor currents represent $\frac{1}{8}$ of the total current in the conductor ring. The sum of the outer conductor rings currents is greater than that of the input current. This can be attributed to manufacturing differences between the coils and noise in the form of electrostatic coupling due to the high rate of rise of voltage. The inner and centre conductor currents are subjected to similar manufacturing differences and electrostatic coupling.

The simulated magnitude response in *Figure 8* shows that at low frequencies the current is evenly distributed, where the outer and inner conductor currents are eight times greater than the current in the centre conductor. As the frequency increases the current tends toward the outer conductors until all the current flows in the outer conductor.

The equivalent circuit, where the current concentrates on the outer conductor ring at high frequencies, is verified, when comparing the measured magnitude in *Figure 6* with the simulated magnitude in *Figure 8*.

The phase angles for the conductor rings are shown in *Figure 9*. At low frequencies the currents are in phase as the resistance is the dominant feature. As the frequency increases, the inductance becomes more dominant and a phase delay on the inner and centre conductor currents is noticeable. At high frequencies the current is limited to the outer resistance and is in phase with the input current.

The lightning impulse response of the conductor rings is shown in *Figures* 10, 11 and 12. It can be seen that the time scales differ considerably. The majority of the current stays on the outer conductor ring, this is due to the high frequency nature of lightning. The currents on the inner conductor ring and the centre conductor are substantially smaller in magnitude and have a delay in time.

In application to LPSs, the current will flow in the down conductors at the outermost part (generally the corners) of a building. Thus the volume enclosed can be considered as the first lightning protection zone (LPZ1). In addition cables run in the centre of a building will experience the least interference from a lightning strike.

6 Conclusion

A skin effect model based on Maxwell's is proposed for the evaluation of the current distribution in a structure. The response of the equivalent circuit is verified by experimental measurements, where it can be seen that the current is concentrated in the outer conductor ring.

A lightning impulse is applied to the circuit and it is seen that the majority of current will flow in the outer conductor ring, with significantly smaller and slower currents on the inner conductor ring and centre conductor.

References

[1] IEC 62305-1 Ed. 1.0. *"Protection against lightning - Part 1: General Principles"*. IEC, Geneva, October 2005.

[2] W. Lewis. "Recommended Power and Signal Grounding for Control and Computer Rooms." *IEEE Transactions on Industry Applications*, vol. 21, no. 6, November/December 1985.

[3] I. Metwally, W. Zischank, and F. Heidler. "Measurement of Magnetic Fields Inside Single- and Double-Layer Reinforced Concrete Buildings During Simulated Lightning Currents." *IEEE Transactions on Electromagnetic Compatibility*, vol. 46, no. 2, pp. 208–221, May 2004.

[4] I. Jandrell, K. Nixon, and J. Van Coller. *Earthing and Lightning Protection*. School of Electrical and Information Engineering, University of the Witwatersrand, August 2005.

[5] G. Celli and F. Pilo. "EMTP Models for Current Distribution Evaluation in LPS for High and Low Buildings." *25th International Conference on Lightning Protection, Rhodes, Greece*, pp. 440–445, September 2000.

[6] G. Ala and M. Di Silvestre. "A Simulation Model for Electromagnetic Transients in Lightning Protection Systems." *IEEE Transactions on Electromagnetic Compatibility*, vol. 44, no. 4, November 2002.

[7] A. Orlandi and F. Schietroma. "Attenuation by a Lightning Protection System of Induced Voltages Due to Direct Strikes to a Building." *IEEE Transactions on Electromagnetic Compatibility*, vol. 38, no. 1, February 1996.

[8] G. Antonini, S. Cristina, and A. Orlandi. "PEEC Modeling of Lightning

Protection Systems and Coupling to Coaxial Cables." *IEEE Transactions on Electromagnetic Compatibility*, vol. 40, no. 4, November 1998.

[9] H. Wheeler. "Formulas for the Skin Effect." *Proceedings of the Institute of Radio Engineers*, vol. 30, September 1942.

[10] C. Yen, Z. Fazarinc, and R. Wheeler. "Time-Domain Skin-Effect Model for Transient Analysis of Lossy Transmission Lines." *Proceedings of the IEEE*, vol. 70, no. 7, July 1982.

[11] J. Kraus. *Electromagnetics*. McGraw-Hill, Inc, fourth ed., 1991.

[12] I. Jandrell. *Attenuation of Very Fast Transients in SF_6 Insulated High Voltage Busducts. Theoretical and Experimental Considerations of the Effect of a Ferromagnetic Coating Applied to the Busbars*. PhD Thesis, University of the Witwatersrand, 1990.

[13] A. Sowa. "Surge Current Distribution in Building During a Direct Lightning Stroke." *IEEE International Symposium on Electromagnetic Compatibility*, 1991.

[14] A. Phillips, G. Grobbelaar, C. Pritchard, R. Melaia, and I. Jandrell. "Development of a Rogowski Coil to Measure Lightning Current Impulses." *SAIEE Transactions*, 1996.

[15] R. Frentzel. "Use of Similarity Relations in the Analysis of Lightning-Induced Transient Phenomena." *European Transactions on Electric Power*, vol. 7, no. 3, May/June 1997.

A Lightning Stroke Parameters

The lightning short stroke parameters are defined in *Figure A.1* [1]. The rise time τ_1 is the time from 10 % to 90 % peak value, the stroke duration τ_2 is the time for the pulse to fall to 50 % of its peak value [1]. The values for 50 % occurence of a number of different lightning strokes are listed in *Table A.1* [1].

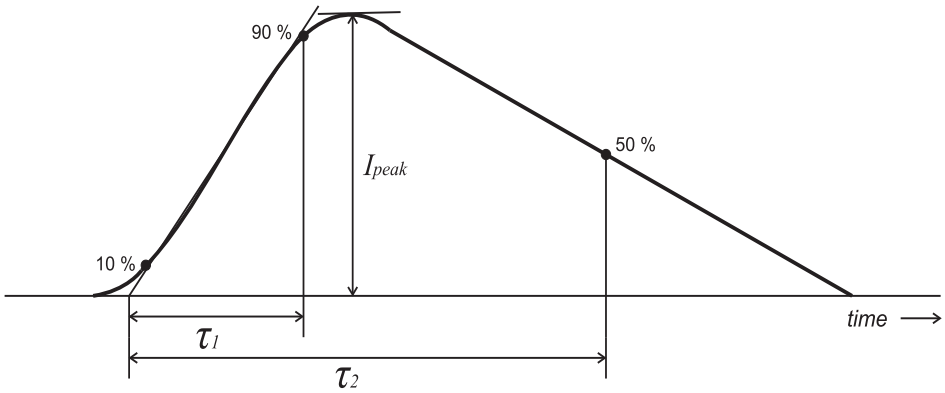

Figure A.1: Lightning short stroke parameters

Table A.1: Lightning short stroke parameters from IEC 61305-1

Parameter	**First negative**	**Subsequent negative**	**First positive**
$\boldsymbol{I}$ (kA)	20	11.8	35
$\boldsymbol{di/dt}$ $(kA/\mu s)$	24.3	39.9	2.4
$\tau_{\mathbf{1}}$ (μs)	5.5	1.1	22
$\tau_{\mathbf{2}}$ (μs)	75	32	230

References

[1] IEC 62305-1 Ed. 1.0. *"Protection against lightning - Part 1: General Principles"*. IEC, Geneva, October 2005.

B Lightning Protection

Lightning protection is required to reduce the risk of damage to equipment or valuables, loss of service and loss of life. The need for lightning protection and the level of protection is determined where these risks are greater than the acceptable risks [1].

Four lightning protection levels are defined according to the acceptable risk (or acceptable number of strikes to a building). A minimum and maximum value is described for each level. The minimum value is used in defining the rolling sphere radius in order to define lightning protection zones [1].

The lightning protection system (LPS) consists of both external and internal lightning protection [1, 2].

B.1 External lightning protection system

The external LPS consists of [1, 2]:

- **air termination**, which has the purpose of intercepting the lightning strike and preventing damage to the building.
- **down conductors**, which conduct the intercepted lightning current to the earth termination.
- **earth termination**, which has the purpose of dissipating the lightning current into the earth.

The external LPS alone does not provide sufficient protection. Additional protection in the form of screens, wiring routing, equipotential bonding and surge protection are used and make up the internal lightning protection system [1, 2, 3].

B.2 Internal lightning protection system

Equipotential bonding, as part of the internal lightning protection system, is used to prevent damage to sensitive electrical and electronic equipment due to differential voltages [1, 2, 4].

Equipotential bonding is implemented by means of bonding bars, cables or reference grids. Due to the transient nature of lightning, the inductance between equipment presents the threat of high differential voltages. Where equipment is close together short individual cables may be used. However multiple parallel paths are required where the equipment is further apart. The multiple paths reduce the impedance between the equipment and reduce the differential voltage between the equipment [1, 4].

A zero signal reference grid (ZSRG) is a metallic grid on which all equipment is bonded. The grid provides an equal voltage across the platform. The impedance between any two points on the grid is small enough that any surge currents are diverted without any ill effect on the equipment [1, 4]

As part of effective and safe grounding, all metallic objects are required to be bonded together and electrically grounded. These objects include pipework, staircases, ventilation, heating and air conditioning ducts and equipment frames. Additionally the external lightning protection system and the metal framework of the building must be bonded together [1, 4]. Where any items cannot be directly bonded, they must be a specified safety distance from any other objects, or must be connected through surge protection devices [1].

The concept of lightning protection zones (LPZ) is defined as successively increasing protection against surges on incoming lines and electromagnetic waves [1, 2]. By implementing screens, bonding of incoming lines and SPD's on incoming lines for each defined zone, an optimal lightning protection solution is found [3].

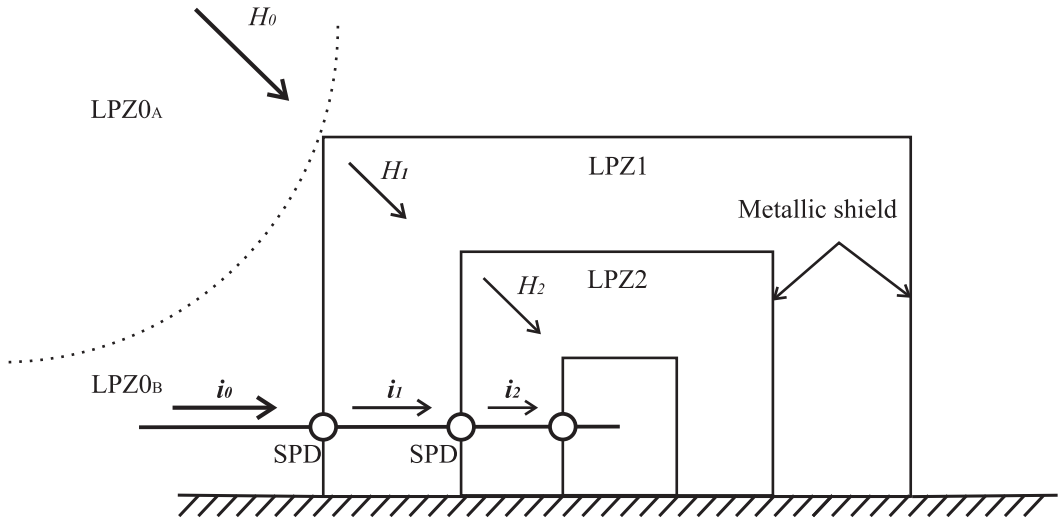

Figure B.1: Lightning protection zones

The zones illustrated in *Figure B.1* are defined [1]:

- **LPZ0**$_A$ - Zone where a direct lightning flash can take place and is exposed to the full electromagnetic field.
- **LPZ0**$_B$ - Zone protected against direct lightning, but is exposed to the full electromagnetic field.
- **LPZ1** - Zone where surge currents on incoming lines are limited by bonding and SPD's, and a screen provides attenuation of the electromagnetic field.
- **LPZn** - Zones where further protection on incoming lines and further attenuation of the electromagnetic field take place.

Lightning protection zones are related to lightning protection levels, where LPZ0$_B$ is defined by the rolling sphere radius, which differs according to the level of protection [1].

B.3 Empirical current distribution in a structure

A current partitioning coefficient is defined as [1]:

$$k_c = \frac{I_k}{I_t} \tag{B.1}$$

The IEC standard provides an empirical relationship for current distribution coefficient in the structure [1]. For a single level building with a mesh air termination and a type B earth electrode, the relationship is given by [1]:

$$k_1 = \frac{1}{2n} + 0.1 + 0.2\sqrt[3]{\frac{c}{h}} \tag{B.2}$$

Where:

c = number of down conductors
c = distance to closest adjacent down conductor [m]
h = height of the down conductor [m]

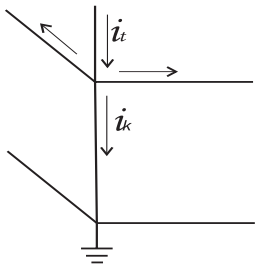

Figure B.2: Current partioning coefficient

It can be seen that the equation is only dependent on the total number of down conductors, and the distance to the closest down conductors. It is independent of the position of the down conductor within the structure, which means it cannot be used to model the current distribution through the entire structure.

References

[1] IEC 62305-1 Ed. 1.0. *"Protection against lightning - Part 1: General Principles"*. IEC, Geneva, October 2005.

[2] I. Jandrell, K. Nixon, and J. Van Coller. *Earthing and Lightning Protection*. School

of Electrical and Information Engineering, University of the Witwatersrand, August 2005.

[3] C. Mazzetti, B. Kuca, and Z. Flisowski. "A Study on the Efficiency of Grid-like Spatial Screens as a Measure of Protection against LEMP." *Journal of Electrostatics*, vol. 60, 2004.

[4] W. Lewis. "Recommended Power and Signal Grounding for Control and Computer Rooms." *IEEE Transactions on Industry Applications*, vol. 21, no. 6, November/December 1985.

C Geometric Modelling

A number of studies relating to lightning protection of full scale buildings [1, 2] and reduced scale buildings [3, 4, 5, 6] have been done. The areas of study include current and voltage distribution in a building [1, 2, 6] and the shielding effect of buildings [3, 4, 5]. These simple structures use only the outer down conductors and do not take into account any down conductors inside the structure.

C.1 Scale factor

The similarity theory is an applied scientific method employed in experimental analysis [7]. Frentzel applies the fundamental principles of the theory to the transient phenomena of lightning [7].

Using the scale factor, q; results from a scaled laboratory experiment are converted to full scale values [7]. A geometric similarity exists where all lengths of the model have the same relation [7]:

$$q = \frac{l}{l'} \tag{C.1}$$

Scale factors for various physical parameters are derived and tabulated [7, 8, 9]:

Table C.1: Scale values applied to model

Physical Quantity	**Scale Factor**
Voltage	$q_V = q$
Current	$q_I = q$
Time	$q_T = q$

C.2 Geometric model

Zischank et al. apply a lightning impulse to a 1:6 scale model, in order to evaluate the concept of lightning protection zones [3, 8, 9]. The model is developed to investigate the shielding effect of single and double layer reinforced concrete buildings. The model consists of only steel rods and steel mesh, and not of concrete as it has no significant effect on shielding [3]. The building model is setup at 90° to normal and surrounded by eight copper return conductors. The symmetrical arrangement of the conductors cancels the the magnetic field at the centre, allowing for an even distribution of current in the structure [3].

Three current impulses are applied to the structure, representing the positive strike, the first negative strike and the subsequent negative strike [3]. The impulses are additionally applied at different strike points; the corner, the mid edge and the middle of the cage [3].

The experiment yields that the strike point at the centre produces a higher voltage due to the even distribution of current through the structure and a strike in the corner gives the highest magnetic fields and derivatives [3]. With the double cage, a shielding improvement from 9.5 to 12 dB for magnetic field derivatives and from 3 to 7 dB for magnetic fields is found [3].

References

[1] S. Visacro, A. Soares Jr., M. Vale, and M. Schroeder. "Evaluation of Current and Potential Distribution for Lightning Protection Systems Including the Behavior of Grounding Electrodes." *25th International Conference on Lightning Protection, Rhodes, Greece*, pp. 464–468, September 2000.

[2] S. Kuramoto, M. Sato, and M. Ohta. "Surge Current and Voltage Distribution in a Reinforced Concrete Building Caused by Direct Lightning Stroke." *IEEE International Symposium on Electromagnetic Compatibility*, 1991.

[3] I. Metwally, W. Zischank, and F. Heidler. "Measurement of Magnetic Fields Inside Single- and Double-Layer Reinforced Concrete Buildings During Simulated Lightning Currents." *IEEE Transactions on Electromagnetic Compatibility*, vol. 46, no. 2, pp. 208–221, May 2004.

[4] M. Santos and J. Paulino. "Lightning Induced Voltages in a Loop Inside a Building." *25th International Conference on Lightning Protection, Rhodes, Greece*, pp. 272–277, September 2000.

[5] T. Milagres, O. Miranda, J. Paulino, and C. Barbosa. "The Lightning Shielding Effect of Buildings: A Reduced Model Study." *27th International Conference on Lightning Protection, Avignon, France*, 2004.

[6] A. Sowa. "Surge Current Distribution in Building During a Direct Lightning Stroke." *IEEE International Symposium on Electromagnetic Compatibility*, 1991.

[7] R. Frentzel. "Use of Similarity Relations in the Analysis of Lightning-Induced Transient Phenomena." *European Transactions on Electric Power*, vol. 7, no. 3, May/June 1997.

[8] W. Zischank, F. Heidler, J. Wiesinger, K. Stimper, A. Kern, and M. Seevers. "Magnetic Fields and Induced Voltages inside LPZ 1 Measured at a 1:6 Scale Model Building." *27th International Conference on Lightning Protection, Avignon, France*, 2004.

[9] A. Kern, F. Heidler, M. Seevers, and W. Zischank. "Magnetic Fields and Induced Voltages in case of a Direct Strike - Comparison of Results obtained from Measurements at a Scaled Building to those of IEC 62305-4." *27th International Conference on Lightning Protection, Avignon, France*, 2004.

D Modelling

A number of models have been developed to predict the performance of lightning protection systems. A number of these studies use a circuital approach [1, 2, 3, 4]. These models are largely based on the inductance equations found in Grover [5]. An alternative approach is the field model approach [6, 7, 8]. Both of these approaches are used to model simple structures, generally consisting only of outer down conductors. A model based on the geometry of the structure must be used to correctly define the distribution of current in the structure.

D.1 Skin effect

The skin effect is the tendency of time-varying currents to crowd or penetrate only the surface of a conductor. Skin, or penetration, depth is dependent on the frequency of the applied waveform and on the parameters of the conductor [9].

Current density in a conductor due to skin effect can be derived from Maxwell's equations and is given by [9, 10]:

$$\mathbf{J} = J_0 e^{-(1+j)\frac{x}{\delta}} \tag{D.1}$$

and skin depth, δ, is given by [9, 10]:

$$\delta = \frac{1}{\sqrt{2\pi f \mu_r \mu_0 \sigma}} \tag{D.2}$$

Where:

f = frequency [Hz]
μ_0 = permeability of free space [H.m^{-1}]
μ_r = relative permeability
σ = conductivity [S.m^{-1}]

The internal inductance is the part of the total inductance which is caused by the magnetic flux within the conductive medium [9]. Wheeler proposes that internal impedance can be represented by distributed circuit elements, consisting of conductances and inductances [9].

At low frequencies, the current flowing in a conductor is distributed uniformly across the cross sectional area of the conductor. The resistance and internal inductance will be

constant [9, 11].

At higher frequencies, the current is concentrated near the surface of the conductor. The resistance of the conductor increases by $\sqrt{f}$, whereas the internal inductance decreases by $\frac{1}{\sqrt{f}}$ [11].

D.2 Partial element equivalent circuit

Ruehli developed an approach to calculate the inductances of complex circuit environments, based on partial inductances [12]. Weeks et al. use a similar approach to account for the skin effect in rectangular conductors [13].

Ruehli extended the partial inductance approach to 3 dimensional multiconductor lines, developing the partial element equivalent circuit (PEEC) model [14].

The integral equation approach begins by summing all sources of electric field within a conductor [14]:

$$\mathbf{E}(\mathbf{r},\omega) = \frac{\mathbf{J}(\mathbf{r},\omega)}{\sigma} + j\omega\mathbf{A}(\mathbf{r},\omega) + \nabla\Phi(\mathbf{r},\omega) \tag{D.3}$$

The vector potential relates the inductance to geometry [12]. For M conductors the vector potential is given by [14]:

$$\mathbf{A}(\mathbf{r},\omega) = \sum_{m=1}^{M} \frac{\mu}{4\pi} \int_{v'_m} \frac{\mathbf{J}(\mathbf{r},\omega)}{|\mathbf{r}-\mathbf{r}'|} dv' \tag{D.4}$$

The scalar potential for M conductors is given by [14]:

$$\Phi(\mathbf{r},\omega) = \sum_{m=1}^{M} \frac{1}{4\pi\epsilon} \int_{v'_m} \frac{\rho(\mathbf{r},\omega)}{|\mathbf{r}-\mathbf{r}'|} dv' \tag{D.5}$$

By substituting equations D.4 and D.5 into equation D.3, where the applied field E_0 is 0 [14]:

$$0 = \sum_{m=1}^{M} \sigma\mathbf{E} + \sum_{m=1}^{M} \frac{\mu}{4\pi} \int_{v'} \frac{\mathbf{J}(\mathbf{r},\omega)}{|\mathbf{r}-\mathbf{r}'|} dv' + \sum_{m=1}^{M} \frac{1}{4\pi\epsilon} \int_{v'} \frac{\rho(\mathbf{r},\omega)}{|\mathbf{r}-\mathbf{r}'|} dv' \tag{D.6}$$

Where the terms are resistive, inductive and capacitive voltage drops respectively [14].

Antonini et al. propose the use of these equations in the development of a PEEC model of a lightning protection system, where each conductive part of the LPS is divided into cells whose length is far less than the wavelength of the highest frequency applied to the system. Each branch takes into account the mutual magnetic and electric coupling [15].

The equivalent circuit for M inductive segments is given by [15]:

$$V_j - V_k - (R_n + j\omega L_{pnn})I_{Ln} - \sum_{m=1}^{M} j\omega L_{pnm} I_{Lm} = V_{sn} \tag{D.7}$$

Where:

$V_j - V_k$ = voltage across branch [V]
R_n = resistance [Ω]
L_{pnn} = self inductance of branch n [H]
I_{Ln} = current in branch n [A]
L_{pn} = mutual inductance of branch m [H]
I_{Lm} = current in branch m [A]

The partial inductances are given by [15]:

$$L_{pmk} = \begin{array}{ll} L_{pskk} - \frac{j\beta\mu_0}{2\pi} l_k^2 & k = m \\ L_{psmk} e^{-j\beta|r_k - r_m|} & k \neq m \end{array} \tag{D.8}$$

Where:

l_k = length of cell k [m]
L_{psmk} = the static partial inductance
β = the propagation constant

This model is applied to a four downconductor structure; more complex models have not been verified with this model [15].

D.3 Skin effect in a circular conductor

Yen, Fazarinc and Wheeler describe a model for skin effect in a coaxial cable based on Maxwell's equations [16]. The conductor is divided into M concentric rings (*Figure D.1*) and a circuit model (*Figure D.2*) consisting of M partial resistors and $M-1$ partial inductors is developed [16].

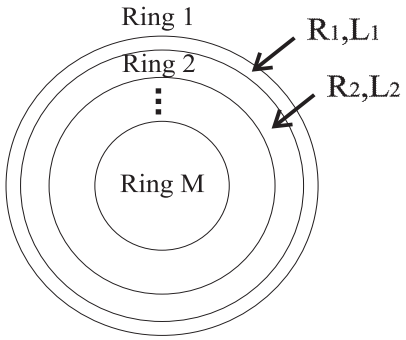

Figure D.1: Concentric rings of a conductor

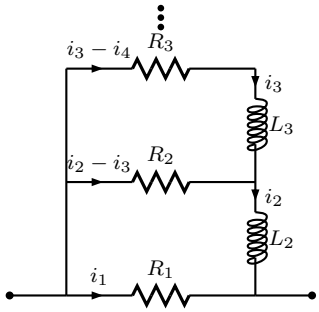

Figure D.2: Skin effect equivalent circuit model

In a the conductor the conductivity is sufficiently high that the displacement current density can be ignored. Faraday's law is given by [16, 17]:

$$\nabla \times \mathbf{J} = -\mu\sigma \frac{\partial \mathbf{H}}{\partial t} \tag{D.9}$$

Ampere's law is given by [16, 17]:

$$\nabla \times \mathbf{H} = \mathbf{J} \tag{D.10}$$

The line integral of the magnetic field is equal to the enclosed current [16]:

$$I(r,t) = 2\pi r H(r,t) \tag{D.11}$$

Combining the previous equations [16]:

$$\frac{\partial J(r,t)}{\partial r} = \frac{\mu\sigma}{2\pi r}\frac{\partial I(r,t)}{\partial t} \tag{D.12}$$

Dividing the conductor into M rings as shown in figure *Figure D.1*, where $i = 1$ is the outermost ring and $i = M$ is the innermost ring, an approximated equation is given by [16]:

$$\frac{J_{i-1} - Ji}{r_{i-1} - r_i} = \frac{\mu\sigma}{2\pi r_i}\frac{dI_i(t)}{dt}, \qquad i = 2, 3..., M \tag{D.13}$$

The current density in a ring is equal to the difference in the enclosed current divided by the area and is given by [16]:

$$J_i = \frac{I_i - I_{i+1}}{A_i}, \qquad i = 1, 2, ..., M \tag{D.14}$$

Substituting equation D.14 into equation D.13 and solving, the resulting equation is given by [16]:

$$R_{i-1}(I_{i-1} - I_i) - R_i(I_i - I_{i+1}) = L_i\frac{dI_i}{dt}, \qquad i = 2, 3, ..., M \tag{D.15}$$

The partial resistances and partial inductances are given by [16]:

$$R_i = \frac{1}{A_i\sigma} \tag{D.16}$$

$$L_i = \frac{\mu(r_{i-1} - r_i)}{2\pi r_i} \tag{D.17}$$

The partial elements are related to the conductivity and permeability [16]. The partial elements form parallel paths, approximating a solution of the skin effect differential equations [18]. For direct current, the impedance reduces to the parallel combination of the resistors, the current distribution is uniform. At higher frequencies the transient current distribution is biased toward the outer rings, due to the presence of partial inductance [16]. The resistance at very high frequencies is limited to the resistance of the outermost ring, since there is no internal flux [18].

A similar approach is taken to include non conductive rings. Faraday's law is given by [17]:

$$\nabla \times \mathbf{E} = -\mu \frac{\partial \mathbf{H}}{\partial t} \tag{D.18}$$

As before:

$$\frac{\partial E(r,t)}{\partial r} = -\frac{\mu}{2\pi r}\frac{\partial I}{\partial t} \tag{D.19}$$

which can be approximated by:

$$E_{i-1} - E_i = \frac{\mu(r_{i-1} - r_i)}{2\pi r_i}\frac{dI_i}{dt} \tag{D.20}$$

From Ohm's law at a point the electric field in a conductor is related to the current density by [17]:

$$\begin{aligned} E_i &= \frac{J_i}{\sigma} \\ &= \frac{I_i - I_{i+1}}{\sigma A_i} \\ &= R_i(I_i - I_{i+1}) \end{aligned} \tag{D.21}$$

For a non-conductive ring the electric field is related to the displacement current density by [17]:

$$\begin{aligned} E_i &= \frac{J_i}{j\omega\epsilon} \\ &= \frac{I_i - I_{i+1}}{j\omega\epsilon A_i} \\ &= -jX_c(I_i - I_{i+1}) \end{aligned} \tag{D.22}$$

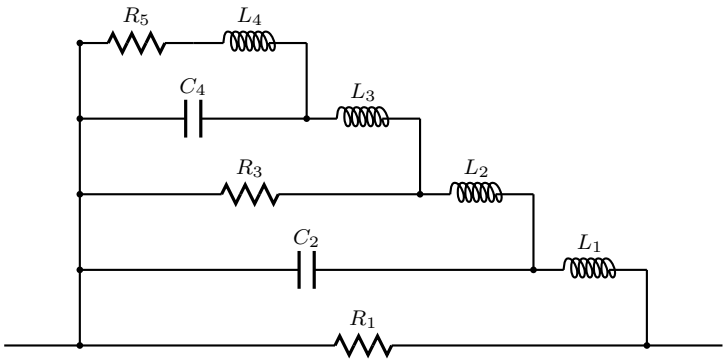

Figure D.3: Skin effect equivalent circuit for a conductor with non conducting layers

The partial resistance and capacitance are derived from equations D.21 and D.22, and the partial inductance is as before (equation D.17). A conductor with alternating conducting and non conducting layers is representing by the equivalent circuit in *Figure D.3*.

References

[1] Q. Zhou and Y. Du. "Using EMTP for Evaluation of Surge Current Distribution in Metallic Gridlike Structures." *IEEE Transactions on Industry Applications*, vol. 41, no. 4, July/August 2005.

[2] W. Bin, Z. Yu-dong, Z. Dong, and F. Zheng-cai. "Discussion on the Equipotential Bonding in Buildings Considering the Situation of a Direct Lightning Stroke." *Proceedings of the XIVth International Symposium on High Voltage Engineering, Beijing, China*, August 2005.

[3] G. Celli and F. Pilo. "EMTP Models for Current Distribution Evaluation in LPS for High and Low Buildings." *25th International Conference on Lightning Protection, Rhodes, Greece*, pp. 440–445, September 2000.

[4] C. Buccella and A. Orlandi. "An Efficient Technique for the Evaluation of Lightning-Induced Voltage in a Cylindrical Vessel Containing Charged Oil." *IEEE Transactions on Industry Applications*, vol. 39, no. 2, March/April 2003.

[5] F. Grover. *Inductance Calculations Working Formulas and Tables*. Dover Publications, Inc., 1964.

[6] S. Miyazaki and M. Ishii. "Lightning Current Distribution Inside of Directly Hit Building." *Proceedings of the XIVth International Symposium on High Voltage Engineering, Beijing, China*, August 2005.

[7] G. Ala and M. Di Silvestre. "A Simulation Model for Electromagnetic Transients in Lightning Protection Systems." *IEEE Transactions on Electromagnetic Compatibility*, vol. 44, no. 4, November 2002.

[8] A. Orlandi and F. Schietroma. "Attenuation by a Lightning Protection System of Induced Voltages Due to Direct Strikes to a Building." *IEEE Transactions on Electromagnetic Compatibility*, vol. 38, no. 1, February 1996.

[9] H. Wheeler. "Formulas for the Skin Effect." *Proceedings of the Institute of Radio Engineers*, vol. 30, September 1942.

[10] U. Inan and A. Inan. *Engineering Electromagnetics*. Addison Wesley Longman, Inc, 1999.

[11] G. Antonini, A. Orlandi, and C. Paul. "Internal Impedance of Conductors of Rectangular Cross Section." *IEEE Transactions on Microwave Theory and Techniques*, vol. 47, no. 7, July 1999.

[12] A. Ruehli. "Inductance Calculations in a Complex Integrated Circuit Environment." *IBM Journal of Research and Development*, vol. 16, September 1972.

[13] W. Weeks, L. Wu, M. McAllister, and A. Singh. "Resistive and Inductive Skin Effect in Rectangular Conductors." *IBM Journal of Research and Development*, vol. 23, no. 6, November 1979.

[14] A. Ruehli. "Equivalent Circuit Models for Three-Dimensional Multiconductor Systems." *IEEE Transactions on Microwave Theory and Techniques*, vol. 22, no. 3, March 1974.

[15] G. Antonini, S. Cristina, and A. Orlandi. "PEEC Modeling of Lightning Protection Systems and Coupling to Coaxial Cables." *IEEE Transactions on Electromagnetic Compatibility*, vol. 40, no. 4, November 1998.

[16] C. Yen, Z. Fazarinc, and R. Wheeler. "Time-Domain Skin-Effect Model for Transient Analysis of Lossy Transmission Lines." *Proceedings of the IEEE*, vol. 70, no. 7, July 1982.

[17] J. Kraus. *Electromagnetics*. McGraw-Hill, Inc, fourth ed., 1991.

[18] I. Jandrell. *Attenuation of Very Fast Transients in SF_6 Insulated High Voltage Busducts. Theoretical and Experimental Considerations of the Effect of a Ferromagnetic Coating Applied to the Busbars*. PhD Thesis, University of the Witwatersrand, 1990.

E Experimental Setup

The structure consists of a number of brass rods arranged in circular rings as illustrated in *Figure E.1.* The outer and inner conductor rings consist of 8 conductors each and there is a single conductor in the centre of the structure. The rings are connected together at the top and the base by copper plates. The copper plate provides an equipotential platform for the down conductors.

The structure is intended to be a reduced scale model of a full scale structure for laboratory experiments. The model is effectively a 1:20 scale model of a real structure.

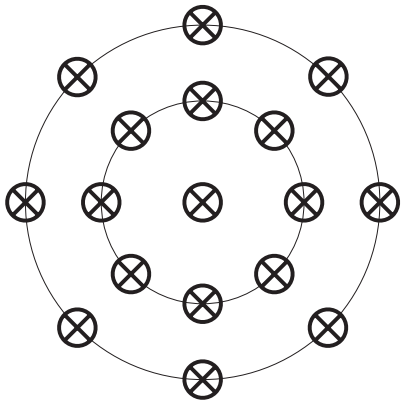

Figure E.1: Conductor ring arrangement

In high frequency applications the return path of the current has an influence on the distribution of the current in the structure. A return path in the form of aluminium mesh surrounds the conductor arrangement, as illustrated in *Figure E.2*, and provides for even distribution of the input current throughout the structure [1, 2].

The structure is constructed from non-ferrous materials to avoid the non linearities associated with the saturation and permeability of ferrous materials. The dimensions of the structure and the radii of the rings are found in both *Figure E.2* and *Table E.1.*

Table E.1: Dimensions of the structure

Parameter	**Value**
Outer radius	14 cm
Inner radius	8.5 cm
Rod radius	3 mm
Rod length	25 cm
Plate width	30 cm

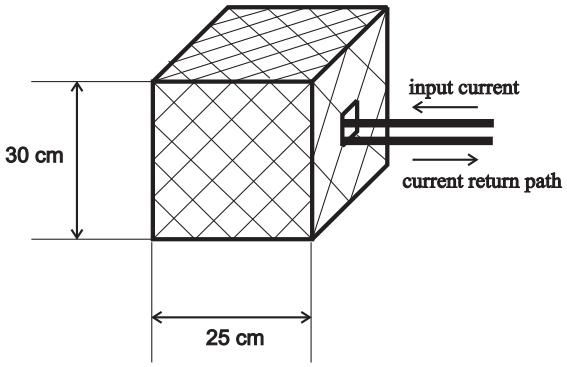

Figure E.2: Test structure setup at an angle of 90° to normal

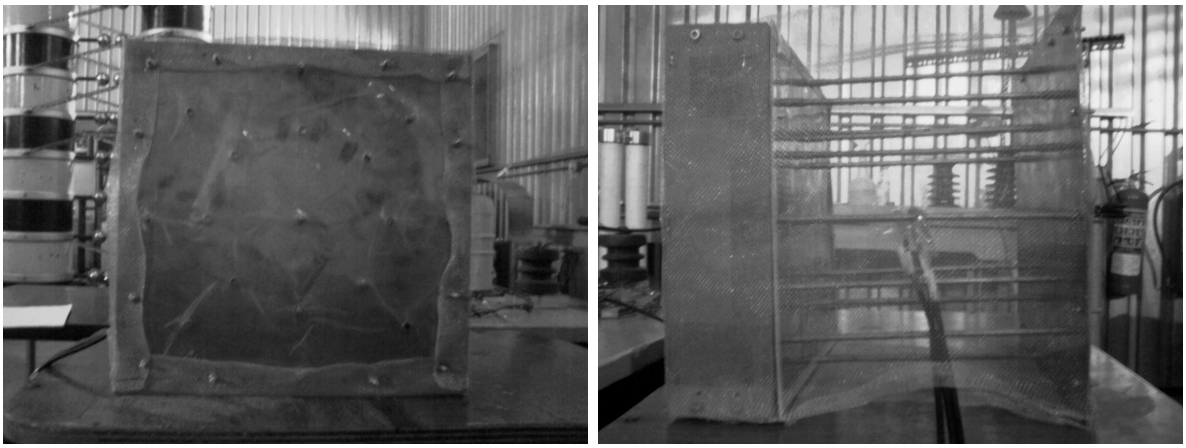

(a) Base view of the structure (b) Side view of the structure

Figure E.3: Pictures of the structure

References

[1] I. Metwally, W. Zischank, and F. Heidler. "Measurement of Magnetic Fields Inside Single- and Double-Layer Reinforced Concrete Buildings During Simulated Lightning Currents." *IEEE Transactions on Electromagnetic Compatibility*, vol. 46, no. 2, pp. 208–221, May 2004.

[2] A. Sowa. "Surge Current Distribution in Building During a Direct Lightning Stroke." *IEEE International Symposium on Electromagnetic Compatibility*, 1991.

F Measurement System

Rogowski coils together with an oscilloscope and MATLAB form the basis of the measurement system. All signal analysis takes place within MATLAB.

Rogowski coils are air cored current sensing devices. The magnetic field produced by a current carrying conductor results in a voltage across the terminals. Due to the air core, the coil does not suffer from the disadvantages of hysteresis or saturation, additionally the bandwidth is dependent on the electrical characteristics of the coil [1, 2, 3].

Physically, Rogowski coils are an application of Ampere's law, given by [2]:

$$i = \oint H.dl \tag{F.1}$$

Where:

H = magnetic field [A/m]
dl = small element along the path [m]

The total magnetic flux linkage is given by [2]:

$$\lambda = \mu_0 nAi \tag{F.2}$$

Where:

μ_0 = permeability of free space [H.m^{-1}]
n = number of turns per metre
A = area [m^2]

The voltage generated across the terminals is given by Faraday's law [2]:

$$\begin{aligned} v &= -\frac{\partial \lambda}{\partial l} \\ &= -\frac{\mu_0 N A}{l}\frac{di}{dt} \end{aligned} \tag{F.3}$$

From the equations above, it is evident that voltage output is proportional to the rate of change of current. The output must be integrated to provide an accurate representation of the current. An active filter requires an op amp and is not suitable due to the high currents and fast waveforms required to be measured. A passive filter consisting of a capacitor and a resistor provides a better solution [1, 2, 3].

The stray capacitance present in Rogowski coils leads to unwanted resonances and may cause large oscillations in the output of the coil. By resistively winding the coil, these resonances are reduced [3]. Resistive wire in the form of nichrome wire is used to wind the coils [1]. For a greater analysis of the coil, an approximate circuit can be developed with the parameters in *Table F.1* [2, 3].

Table F.1: Approximate Rogowski coil parameters

Parameter	**Value**
Area, A	1.96×10^{-3} m^2
Number of turns, N	117
Length, l	77 mm

A large rate of rise of voltage ($\frac{dV}{dt}$) may cause electrostatic interference. This interference can be reduced by means of shielding, however, the electrostatic shielding increases coil capacitance, which reduces the high frequency bandwidth of the coil [4].

Each rogowski coil is connected to an oscilloscope by means of a coaxial cable. Each rogowski coil will have manufacturing differences and the coaxial cable will not have the same length. These differences are compensated for by means of a transfer function [1].

$$T_k(\omega) = \frac{F_k(\omega)}{F_1(\omega)} \tag{F.4}$$

Where:

F_k = frequency response of measurement coil

F_1 = frequency response of reference coil

References

[1] A. Swanson, M. Grant, K. Nixon, and I. Jandrell. "Evaluation of the Lightning Current Distribution in a Scale Model of a Building." *South African Universities Power Engineering Conference (SAUPEC)*, January 2005.

[2] A. Phillips, G. Grobbelaar, C. Pritchard, R. Melaia, and I. Jandrell. "Development of a Rogowski Coil to Measure Lightning Current Impulses." *SAIEE Transactions*, 1996.

[3] A. Phillips, G. Grobbelaar, and I. Jandrell. "The Modelling and Development of a Resistively Wound Rogowski Coil for Measuring Lightning Current Impulses." *23rd International Conference on Lightning Protection*, September 1996.

[4] C. Hewson and W. Ray. "The Effect of Electrostatic Screening of Rogowski Coils Designed for Wide-Bandwidth Current Measurement in Power Electronic Applications." *35th Annual IEEE Power Electronics Specialists Conference*, 2004.

G Results

G.1 Simulated results

A model consisting of 5 concentric rings is used to simulate the current distribution in the structure. The 5-stage equivalent circuit (*Figure G.1*) is developed and implemented in ATP, where:

- R_1 represents the outer conductor ring
- C_2 represents the gap between the outer and inner conductor ring
- R_3 represents the inner conductor ring
- C_4 represents the gap between the inner conductor ring and the centre conductor
- R_5 represents the centre conductor
- L_2 to L_4 represent the partial inductances of each ring.

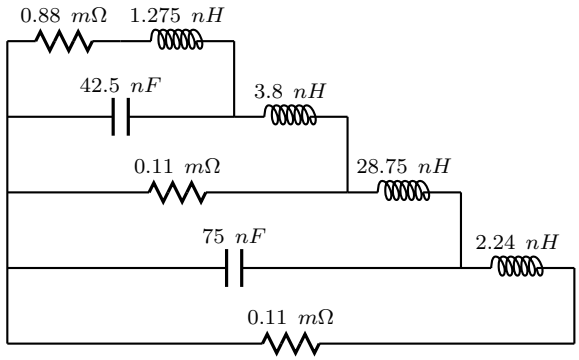

Figure G.1: Approximate skin effect equivalent circuit

The magnitude and phase angle for the different is are shown in *Figures* G.2 and G.3 for the frequency range of 0 Hz to 1 MHz, where the input current is given by:

$$I_{in} = 100sin(2\pi f_0 t) \tag{G.1}$$

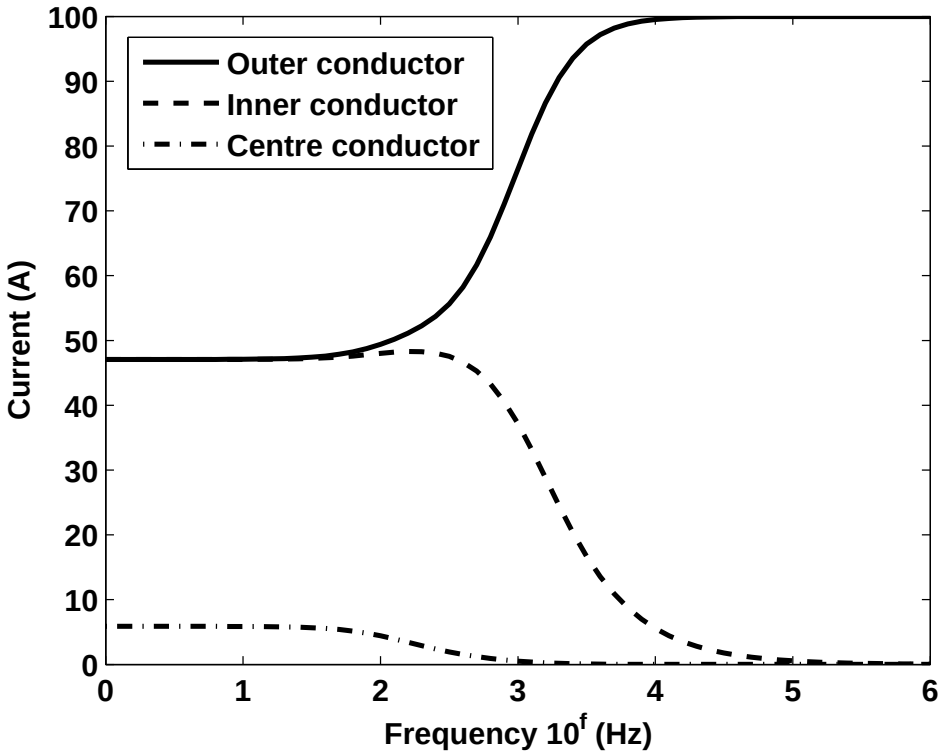

Figure G.2: Magnitude response of the different conductors of the structure

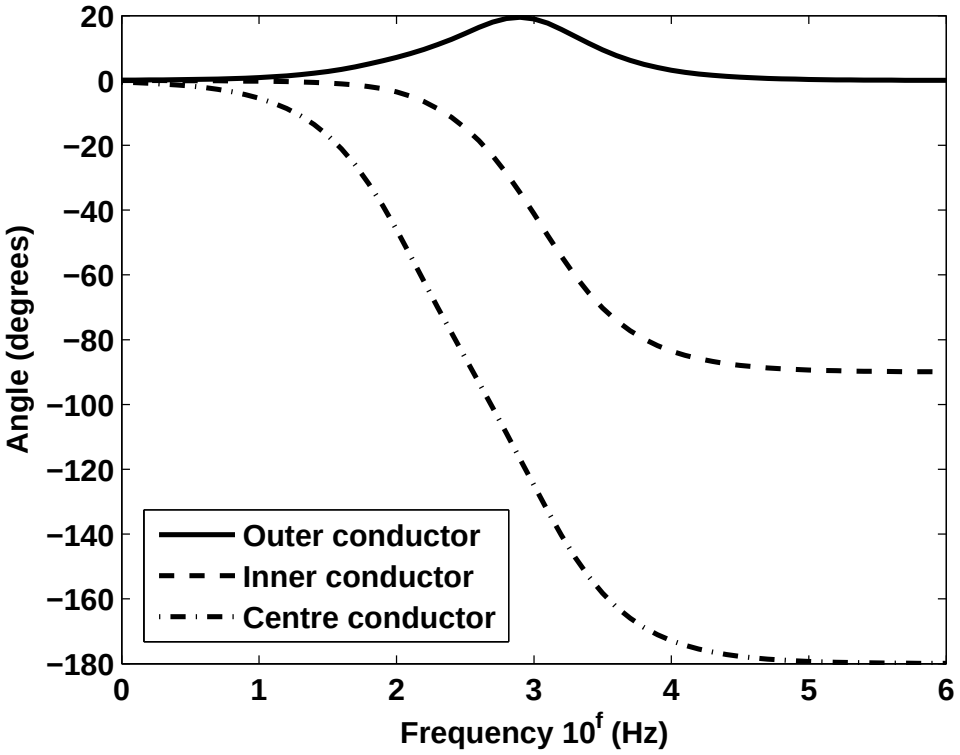

Figure G.3: Phase angle of the different conductors of the structure

A lightning impulse is simulated by means of a Heidler source given by [1]:

$$I = I_{peak} \frac{\left(\frac{t}{\tau_f}\right)^n}{\left(1 + \left(\frac{t}{\tau_f}\right)^n\right)} \exp\left(\frac{t}{\tau_f}\right) \tag{G.2}$$

Where:

I_{peak} = peak current [A]
τ_f = front time [μs]
τ_t = tail time [μs]
n = factor influencing the rate of rise

Since the structure is a 1:20 scale representation of a real structure, the front time and tail time of the impulse must be scaled accordingly [2]. The impulse has the parameters found in the *Table G.1* and the resulting impulse waveforms are found in *Figures* G.4 to G.7. It must be noted that the time scales differ in each figure.

Table G.1: Heidler source parameters

Parameter	**Value**
I_{peak}	100 A
τ_f	0.3 μs
τ_t	3.75 μs
n	2

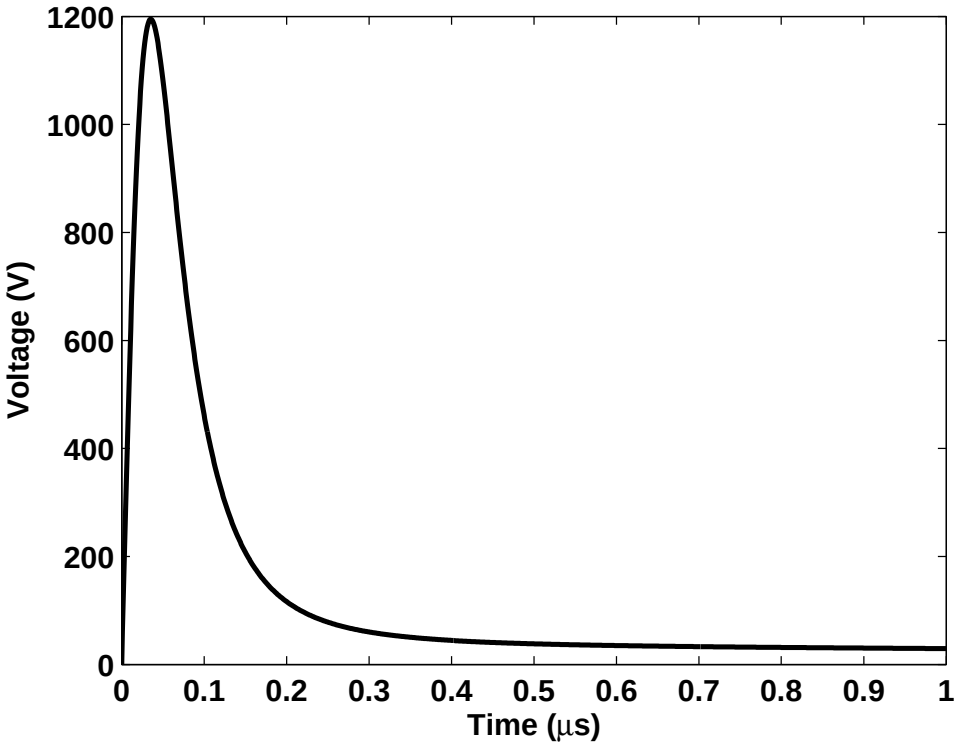

Figure G.4: Voltage impulse

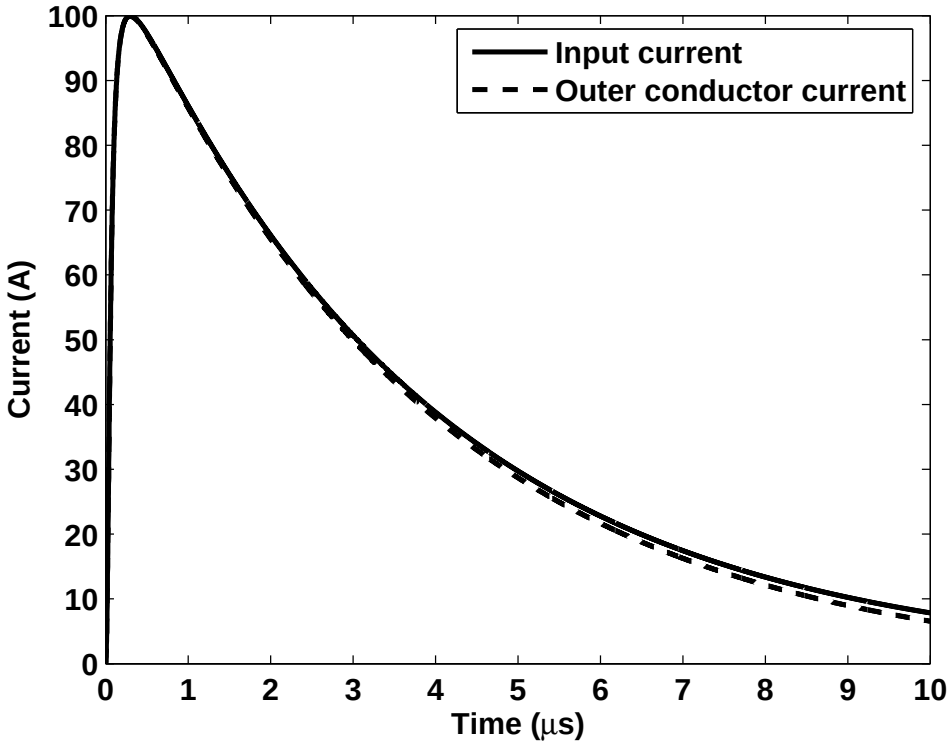

Figure G.5: Impulse response for the outer conductor ring

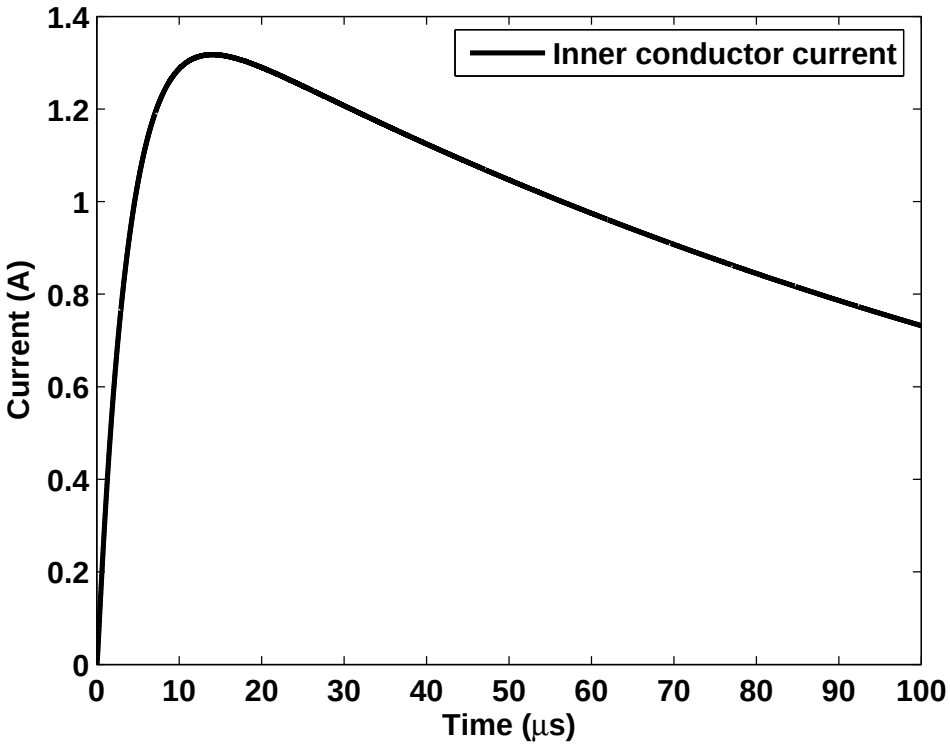

Figure G.6: Impulse response for the inner conductor ring

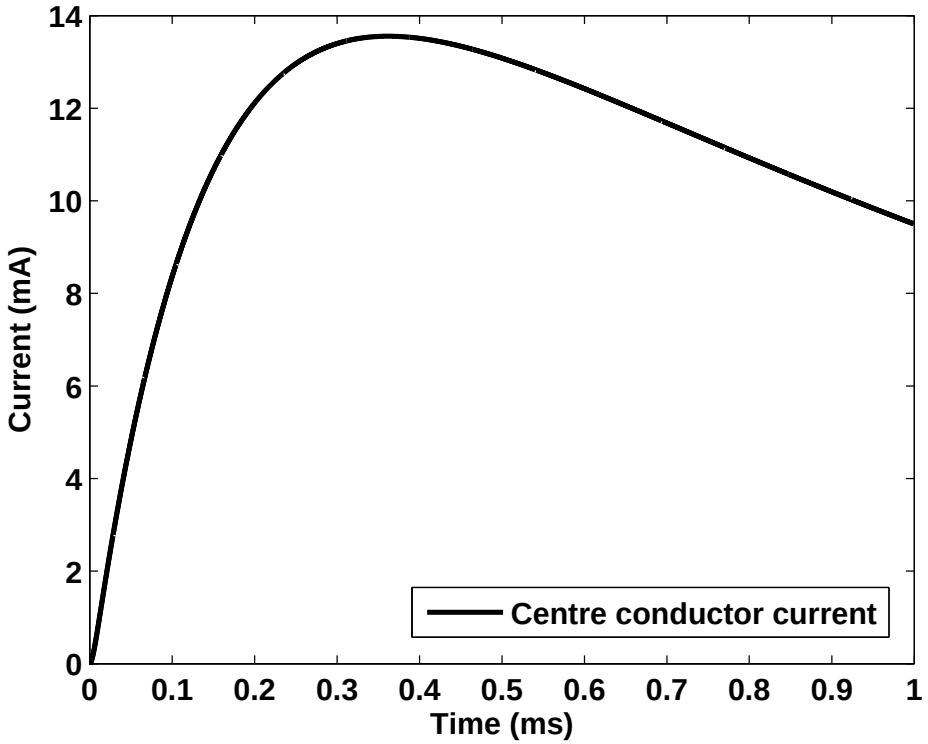

Figure G.7: Impulse response for the centre conductor

G.2 Experimental results

For high frequency measurements the return path of the current has an major influence on the current distribution in the structure due to the inductance. For this reason the return path takes the form of a mesh completely surrounding the structure, this allows for the even distribution of current within each conductor ring [3, 4].

Four current measurements are taken:

- Input current
- Outer conductor current (representing $\frac{1}{8}$ of the total current of the outer conductor ring)
- Inner conductor current (representing $\frac{1}{8}$ of the total current of the inner conductor ring)
- Centre conductor current

Each conductor current is referenced to the input current such that:

$$I_{in} = sin(2\pi f_0 t) \tag{G.3}$$

The output voltage of the Rogowski coil increases with increasing frequency, since this voltage is proportional to the rate of change of current [5]. The ability to measure small currents becomes possible at high frequencies. The measurements are limited to a frequency range from 50 kHz to 1.25 MHz.

The Rogowski coils and coaxial lines are not shielded and are subjected to noise. Additional noise in the form of resonance in the coils is evident at 12.5 MHz. Filters are applied in MATLAB to remove the unwanted noise.

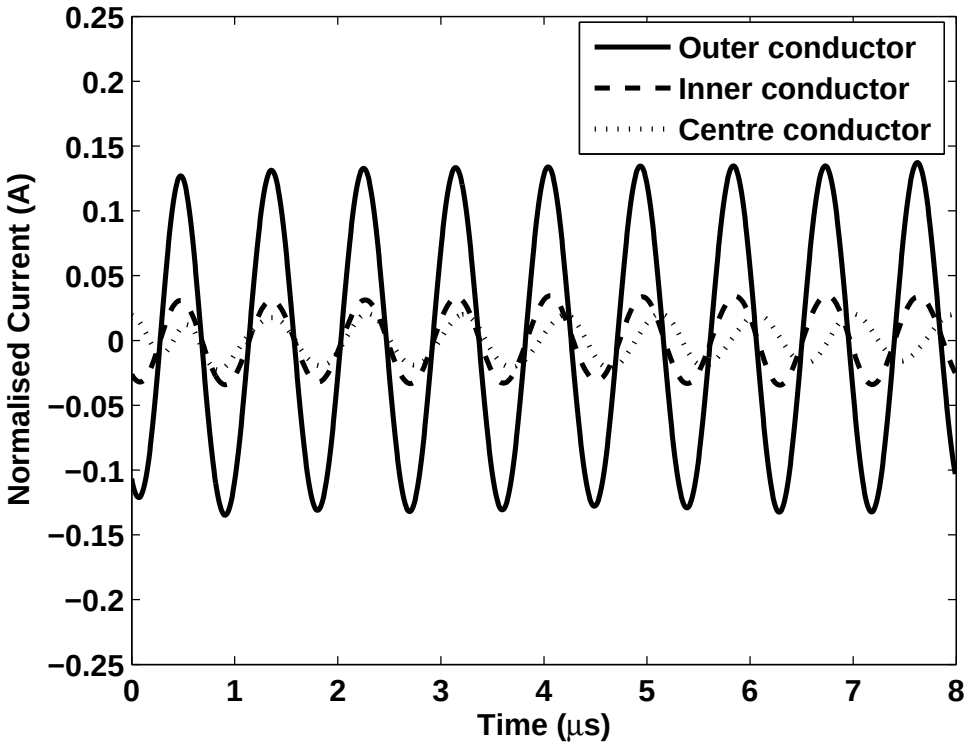

Figure G.8: Measured distribution in the time domain where $f_0 = 1.25$ MHz

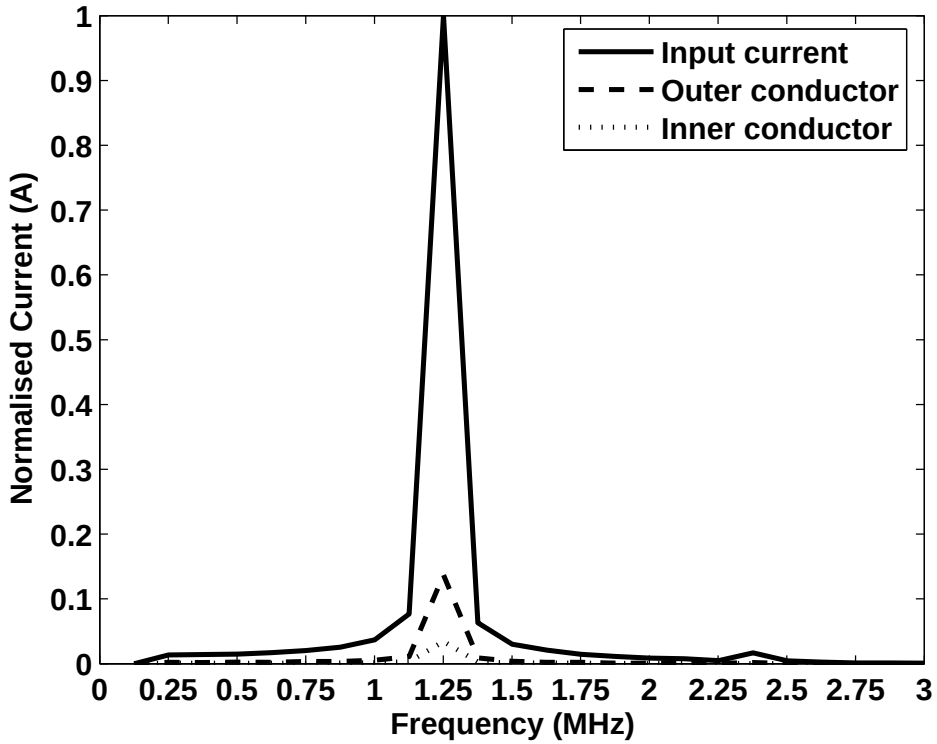

Figure G.9: Measured distribution in the frequency domain where $f_0 = 1.25$ MHz

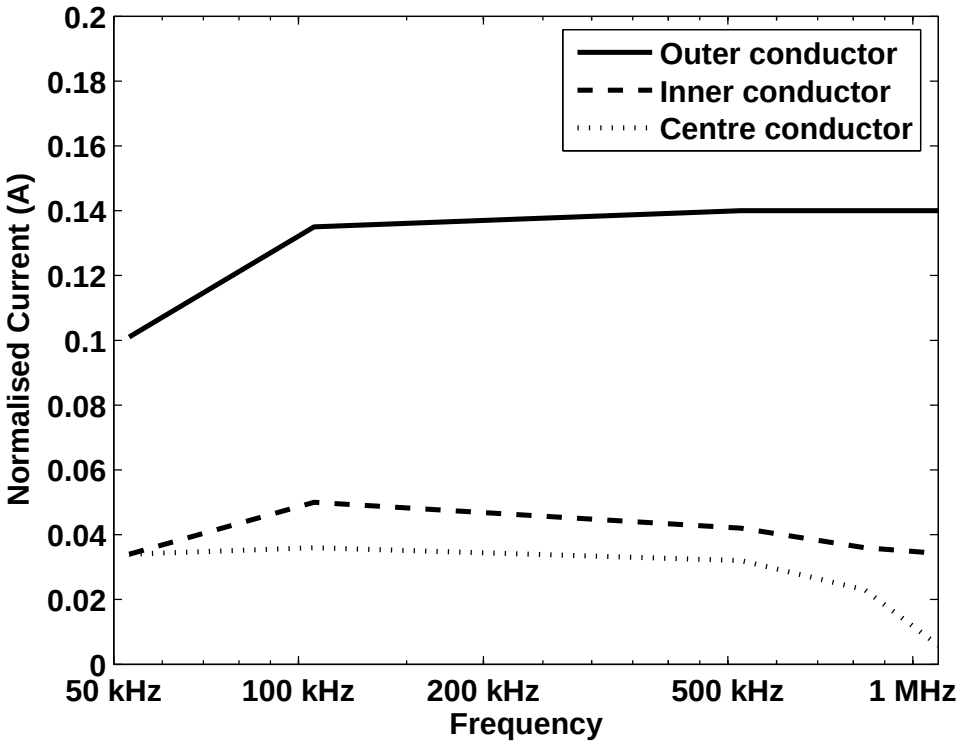

Figure G.10: Measured magnitude of the structure in the frequency domain from $f_0 = 50$ kHz to $f_0 = 1.25$ Mhz

References

[1] J. Van Coller. *An Introduction to EMTP*. University of the Witwatersrand, Department of Electrical Engineering, 1993.

[2] R. Frentzel. "Use of Similarity Relations in the Analysis of Lightning-Induced Transient Phenomena." *European Transactions on Electric Power*, vol. 7, no. 3, May/June 1997.

[3] I. Metwally, W. Zischank, and F. Heidler. "Measurement of Magnetic Fields Inside Single- and Double-Layer Reinforced Concrete Buildings During Simulated Lightning Currents." *IEEE Transactions on Electromagnetic Compatibility*, vol. 46, no. 2, pp. 208–221, May 2004.

[4] A. Sowa. "Surge Current Distribution in Building During a Direct Lightning Stroke." *IEEE International Symposium on Electromagnetic Compatibility*, 1991.

[5] A. Phillips, G. Grobbelaar, C. Pritchard, R. Melaia, and I. Jandrell. "Development of a Rogowski Coil to Measure Lightning Current Impulses." *SAIEE Transactions*, 1996.